Measurement 256 (2025) 118256

Contents lists available at ScienceDirect

Measurement

journal homepage: www.elsevier.com/locate/measurement

Design and initial experimental verification of a high-speed electrodynamic levitation measurement system utilizing modular magnetic field sources and aluminium rails

U. Kemal Ozturk [a,*], Hakki Mollahasanoglu [a,b], Murat Abdioglu [a,c], Halil Ibrahim Okumus [d], Hasan Gedikli [e]

[a] Electromagnetic Guidance and Acceleration Research Group (EMGA), Department of Physics, Faculty of Science, Karadeniz Technical University, 61080 Trabzon, Türkiye
[b] Department of Electrical-Electronics Engineering, Faculty of Engineering and Architecture, Recep Tayyip Erdoğan University, 53100 Rize, Türkiye
[c] Department of Mathematics and Science Education, Faculty of Education, Bayburt University, 69000 Bayburt, Türkiye
[d] Department of Electrical-Electronics Engineering, Faculty of Engineering, Karadeniz Technical University, 61080 Trabzon, Türkiye
[e] Department of Mechanical Engineering, Faculty of Engineering, Karadeniz Technical University, 61080 Trabzon, Türkiye

ARTICLE INFO

Keywords:
Electrodynamic levitation
HTS
Maglev
Permanent magnet

ABSTRACT

This work presents design and development of a modular high-speed electrodynamic levitation (EDL) test system that integrates advanced magnetic field configurations and real-time control capabilities at high operational speeds. The system comprises a rotating aluminium rail and interchangeable magnetic field sources, including permanent magnet array (PMA) and high-temperature superconducting (HTS) bulk, allowing for a variety of experimental configurations. The initial experimental results focused on testing the system through PMA–aluminium rail and HTS–aluminium rail configurations. A key innovation of this system is its modular structure, which allows for easy replacement and reconfiguration of magnetic components and rail geometries. The adaptability of the system enables a thorough investigation of how different magnetic field sources influence magnetic force and dynamic stability at high speeds. Furthermore, the system is fully integrated with a programmable logic controller (PLC) and supervisory control and data acquisition (SCADA) interface, enabling precise real-time monitoring, synchronized control and automatic data acquisition. Experimental results demonstrate the system's capability to measure vertical displacement variations and force fluctuations at different speeds, with resonance effects identified around 145 km/h. The levitation forces of 99 N were measured at a gap of 10 mm, with the PMA at a maximum speed of 283 km/h above an aluminium rail, while it was measured as 16 N with HTS at a vertical gap of 9 mm. This flexible test platform provides a critical foundation for determining the force parameters of the real-scale EDL Maglev technologies and advancing their practical application potential in high-speed transportation.

1. Introduction

Today, transportation systems contribute significantly to economic and social development by enabling both people and property to move efficiently over long distances. With increasing urbanization and environmental concerns, there is a growing need for sustainable, high-speed with comfort and energy efficient transportation solutions. In this scope, magnetic levitation (maglev) technology stands out with its ability to eliminate physical contact between the vehicle and the rail, significantly reducing friction, noise and maintenance costs [1]. In the literature, many studies on Maglev systems have been carried out to date, and research in this field continues intensively today [2,3]. Maglev systems, which offer high-speed travel with minimal environmental impact, have significant potential in the field of transportation. These systems are based on three main technologies: Electromagnetic levitation (EML), electrodynamic levitation (EDL) and High Temperature Superconductor (HTS)-pinning levitation. EML systems utilize the attractive force of electromagnets to levitate a train on a ferromagnetic rail and many studies have been conducted in this field [4–6]. But, EML systems have the disadvantages of high energy consumption, complex control

* Corresponding author.
E-mail address: kozturk6167@gmail.com (U.K. Ozturk).

https://doi.org/10.1016/j.measurement.2025.118256
Received 19 March 2025; Received in revised form 11 June 2025; Accepted 23 June 2025
Available online 24 June 2025

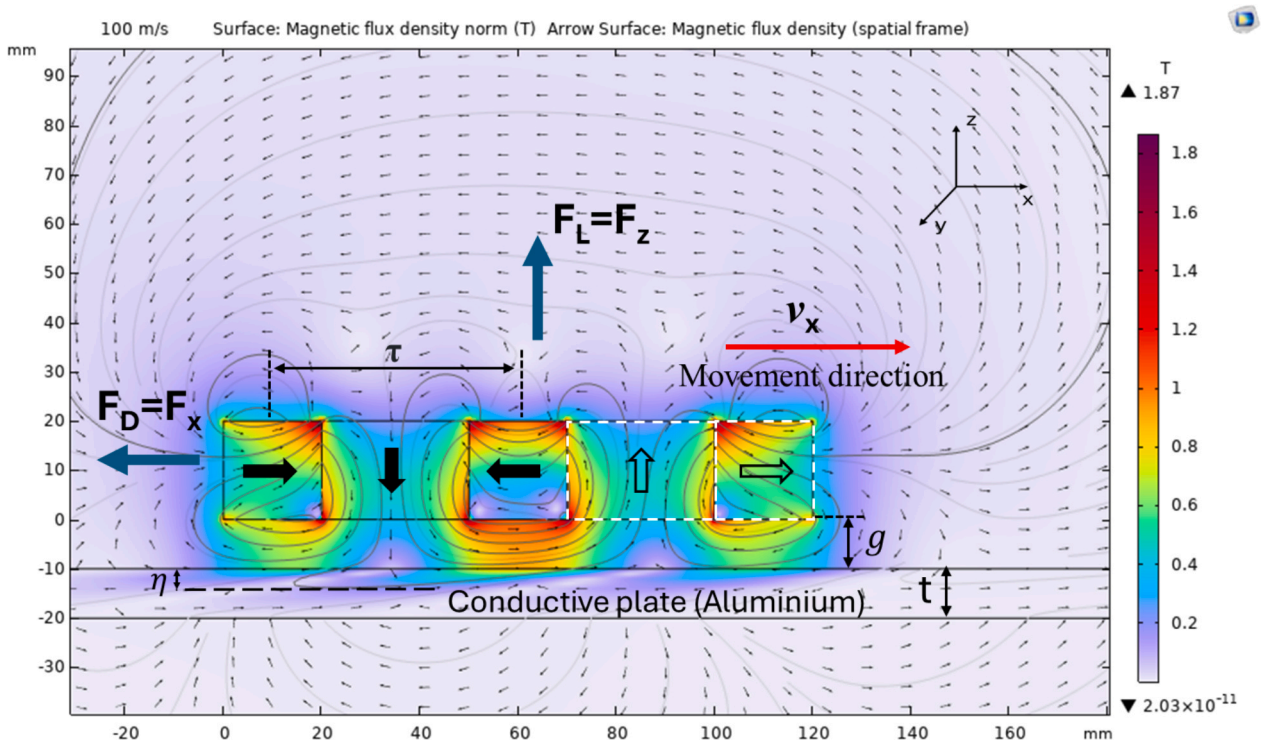

Fig. 1. Schematic illustration of the physical model of the EDL system. Surface plot shows the norm of magnetic flux density (T), while arrow surface represents the B_x and B_y magnetic flux density.

mechanisms and sensitivity to external factors. EDL maglev systems use repulsive magnetic forces based on the eddy current between the conductive track and the magnetic field source in the vehicle, generated by motion, to achieve high-speed, frictionless travel [1,7]. HTS-pinning maglev systems take advantage of the phenomenon of flux pinning, which occurs when superconducting materials trap magnetic field lines generated by the magnetic track constructed with permanent magnets [8].

Many research teams have developed static and dynamic test setups to investigate electromagnetic force parameters between the magnetic field unit and rail configurations [9,10]. A system was designed to perform magnetic levitation force and magnetic stiffness measurements of superconducting samples, considering temperature, measurement speed and time dependencies between 20 K and 300 K [11]. Similar static measurement test systems have been developed that focus on the basic principles of maglev technology, magnetic force relationships and levitation characteristics [6,12–14]. However, these static measurement systems have been limited by the inability to address dynamic effects (e.g. velocity, acceleration) reflecting real operating conditions. Therefore, dynamic measurement systems have been developed to study the dynamic behaviour of Maglev systems [15]. For example, in a study conducted in China, a test system with a side-suspended HTS-permanent magnet array (PMA) with a maximum speed of 150 km/h was built to investigate the dynamic stability at high operating speeds [16]. Liu et al. observed the weakening trend of the levitation force in another system reaching maximum velocity of 135 km/h [17]. Zhuo et al. improved the speed-dependent vibration models in their test study [18] while, Deng et al. evaluated the dynamic stability of HTS maglev train on a circular test track [19]. These measurement systems use circular rail systems instead of linear test rails to achieve the high speeds of real applications on a laboratory scale. For example, measurement system called SCML-03, a speed of 300 km/h was achieved with a 70 kW DC motor driving a 1.5-meter diameter PMA [20]. With a larger diameter vacuum pipeline test prototype, the HTS model vehicle reached a speed of 150 km/h [16]. In these studies, it is seen that the speeds on small radius circular test tracks remain at low levels.

Before implementing high-speed EDL test systems, initial measurements are typically conducted to evaluate system stability under dynamic conditions. These assessments include analysing vibrations [21], speed-dependent displacement variations, and dynamic levitation height fluctuations to ensure reliable operation [22]. In HTS test systems, quasi-static, dynamic, and validation experiments have been conducted to address gaps by measuring the levitation force, magnetostatic stiffness, and damping coefficients of bulk arrays [23]. Similarly, the relationship between levitation force and displacement is examined to determine the system's magnetic stiffness characteristics and overall ride quality [24]. In many test setups, force–displacement hysteresis loops, vibration spectra, and damping properties are measured to identify potential instabilities at high speeds [25]. HTS coils with permanent current, produced within the scope of the HTS magnet development project initiated in 1999, were successfully tested at the Yamanashi Maglev Test Line in 2005, reaching a speed of 553 km/h. [26]; comparative measurements with different guideway types reveal that the levitation performance varies depending on the orientation, gradient and structural distribution of the magnetic field [27]. These analyses play a crucial role in optimizing maglev system design, control strategies, and operational stability for practical applications.

This paper presents a high-speed EDL Maglev measurement system based on eddy current levitation principle. Thanks to its modular magnetic field sources and aluminium rail structure and geometries, the system allows for easy testing of different configurations and determination of their dynamic magnetic force interaction parameters. Different magnetic field sources such as PMA, bulk HTS, and HTS racetrack coil as well as aluminium rails of various thicknesses and geometries can be interchanged within the system, making it possible to comparatively analyse the effects on the magnetic force. Additionally, thanks to the integrated PLC software and SCADA interface, measurements can be taken precisely, the system can be controlled, and the obtained data can be reported, easily. With these features, the study aims to provide a flexible and comprehensive measurement environment for EDL Maglev

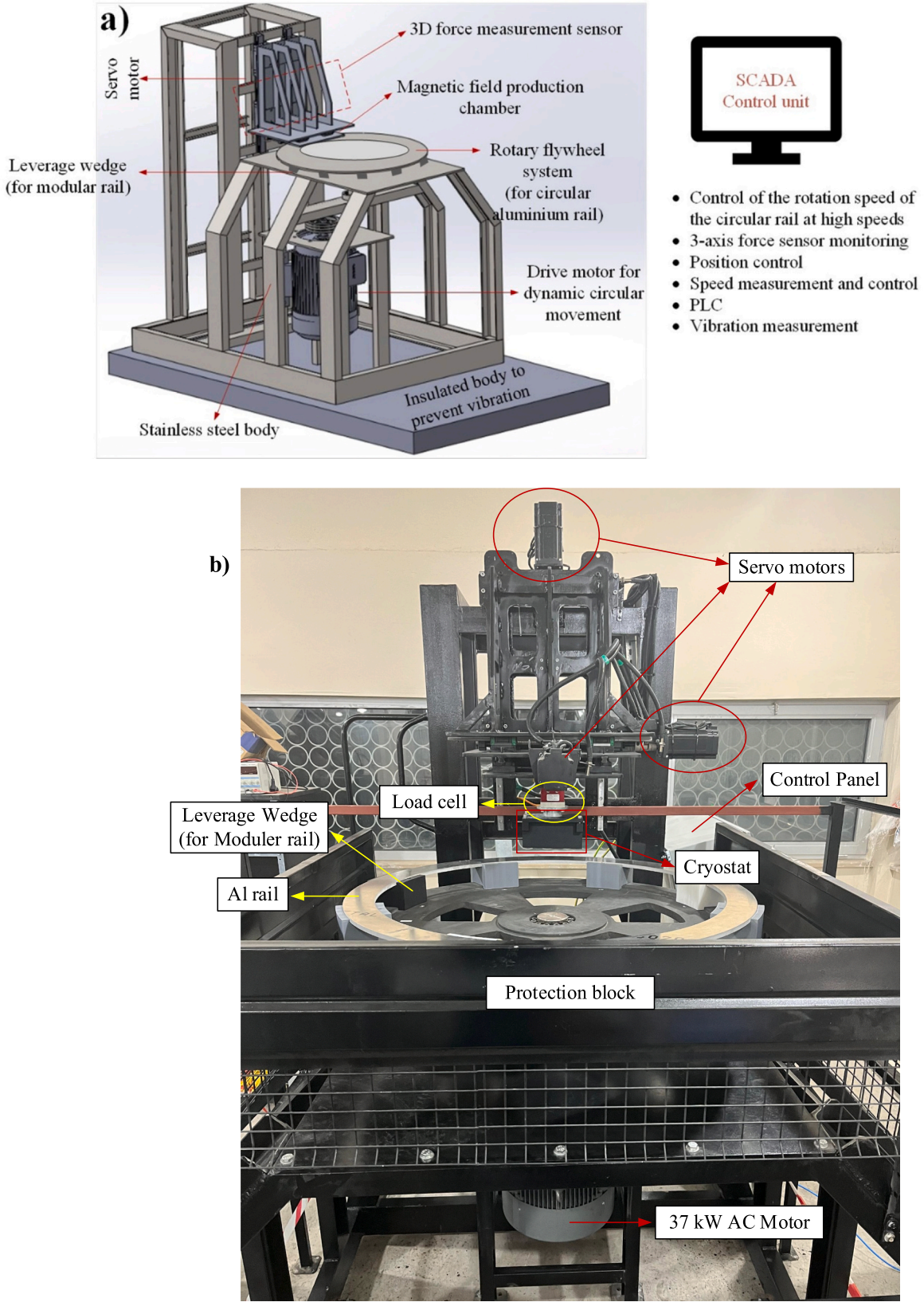

Fig. 2. Schematic view (a) and photograph (b) of the HTS-Aluminium rail EDL measurement system.

test systems.

The rest of the paper is structured in the following manner: section 2 outlines the design of high-speed EDL measurement systems; section 3 presents experimental results and discussions while section 4 reports the concluding remarks.

2. High-speed electrodynamic levitation measurement system design

The development of EDL test systems requires a comprehensive approach that integrates advanced magnetic field sources, precision rail configurations and real-time monitoring capabilities. This chapter presents the key design principles and technical considerations involved in the creation of the modular, high-speed EDL test system we have built. The system is designed to evaluate the dynamic behaviour of the Maglev system under various operational conditions, with a focus on optimizing levitation, stability and efficiency. Using different magnetic field sources such as permanent magnets in PMA, HTS and coil-based configurations with aluminium rails, this test system provides systematic experimental study on real-scale EDL applications. Furthermore, the integration of PLC and SCADA to the fabricated EDL measurement system provides precise control and data acquisition facilitating comprehensive analysis.

2.1. Fundamental principle of electromagnetic force in the EDL system

The levitation phenomenon in the EDL system is based on the interaction between the magnetic flux of the magnetic field source and the eddy currents formed in the conductive plate (aluminium) on which the magnetic field source moves.

The eddy currents and, thus, the electromagnetic force depend on the relative velocity between the onboard magnetic field source unit and the conductive plate. The simplest form of an EDL system and consisted forces in different direction are illustrated in Fig. 1. This figure also illustrates the arrow surface representing the x- and y-components of magnetic flux density (B_x and B_y), and surface plot for the norm of magnetic flux density in T, obtained by a finite element method in COMSOL Multiphysics 6.1 software [7].

In this system, the magnetic field of the PMA induces eddy currents in the conductive plate when the PMA moves on it. These eddy currents subsequently create their own magnetic fields. The repulsive levitation force in a PMA-EDL system results from the interaction between these two magnetic fields. The fundamental physics behind this phenomenon can be explained simply by starting with Faraday's law:

$$\nabla \times \boldsymbol{E} = -\frac{\partial \boldsymbol{B}}{\partial t} \tag{1}$$

Also, considering the moving charge carrier in the conducting plate the Faradays Law can be explained as follows:

$$\boldsymbol{E} = \boldsymbol{v} \times \boldsymbol{B} \tag{2}$$

where E is the electric field created in the conductive plate, v is the velocity of the conductive plate in the x- axis and B is the magnetic flux density (see Fig. 1). Let σ be the electrical conductivity of the plate, then the induced eddy current density, $\boldsymbol{J}$ can be defined as:

$$\boldsymbol{J} = \sigma \boldsymbol{E} \tag{3}$$

Substituting (2) into (3) and assuming the PMA is moving only along the x axis, the induced eddy current is derived as follows [28].

$$\boldsymbol{J} = \sigma(\boldsymbol{v} \times \boldsymbol{B})$$

$$J_x = 0, J_y = -\sigma v B_z, J_z = \sigma v B_y \tag{4}$$

Lorentz Force, F and components; F_x drag force (F_D), F_z levitation force (F_L), and F_y guidance force (F_G) between consisted eddy current in the conductive plate and magnetic field source can be obtained as follows:

$$\boldsymbol{F} = \boldsymbol{J} \times \boldsymbol{B} = \begin{vmatrix} \boldsymbol{i} & \boldsymbol{j} & \boldsymbol{k} \\ 0 & -\sigma v B_z & \sigma v B_y \\ B_x & B_y & B_z \end{vmatrix}$$

$$F_x = F_D = -\sigma v\left(B_z^2 + B_y^2\right)$$

$$F_y = F_G = \sigma v\left(B_x B_y\right)$$

$$F_z = F_L = \sigma v(B_x B_z) \tag{5}$$

It can be said by (5) that to increase the levitation force and decrease drag force simultaneously, B_x is preferred to be maximum while B_z should be minimum.

In addition to the above microscopic explanation of magnetic flux and induced current density in the conductive plate, these forces can be expressed macroscopically by considering the PMA arrangement by Eqs. ((6)–(8)), where B_0 denotes the peak magnetic flux density of the PMA, w is the width of the magnet array, ρ represents the number of pole pairs and τ is the pole pitch (see Fig. 1). Besides, β is the magnetic field decay factor, defined as $\beta = \pi/\tau$, g denotes the air gap between the PMA and the conductive plate and μ_0 is the permeability of free space. One of the key parameters in EDL systems is the skin depth η, which determines the extent to which the magnetic field penetrates the conductive plate. It is defined in Eq. (8), where λ denotes the magnetic pole wavelength.

$$F_z = F_L = \frac{B_0^2 w \rho \tau}{\mu_0} \frac{1}{\beta\eta + 1} e^{-2\beta g} \tag{6}$$

$$F_x = F_D = \frac{B_0^2 w \rho \tau}{\mu_0} \frac{\beta\eta}{\beta\eta + 1} e^{-2\beta g} \tag{7}$$

$$\eta = \sqrt{\frac{\lambda}{\pi \mu \sigma v}} \tag{8}$$

2.2. General description of the measurement system

The developed EDL measurement system allows the measurement of magnetic levitation force, guidance force, and dynamic vibration parameters of different magnetic field source-rail configurations at rotational speeds of 1700 rpm which is equivalent to 320 km/h linear speed. The main components of this test system are a rotating circular rail (modular structure), magnetic field source module (PMA, bulk HTS, and HTS racetrack coil), cryostat, drive and servo motors, force sensors and integrated PLC-SCADA control system.

This measurement system, which is illustrated in Fig. 2, is designed using a 1000 mm diameter circular flywheel instead of the traditional long linear test lines. This structure, which allows high speeds to be achieved in short distances, allows easy replacement of on-board magnetic source units and aluminium rail configurations of different thicknesses and geometries thanks to its modular structure. For the preliminary test measurements, the aluminium rail width is specified as 70 mm. A 37 kW AC motor with high torque capacity and precise speed control is used to ensure the stability of the system at high speeds. The power transmission from the motor to the flywheel (for circular aluminium rail) is accomplished by a belt-pulley system that reduces vibrations and stabilizes torque transmission. Also, the drive motor is mounted directly to ground separately the 3D force measurement unit in order to reduce the mechanical vibration caused by drive motor. Fig. 2 shows a schematic representation and photograph of the high-speed EDL measurement system.

2.3. Design of portable magnetic field sources

The magnetic field source used in the EDL measurement system is

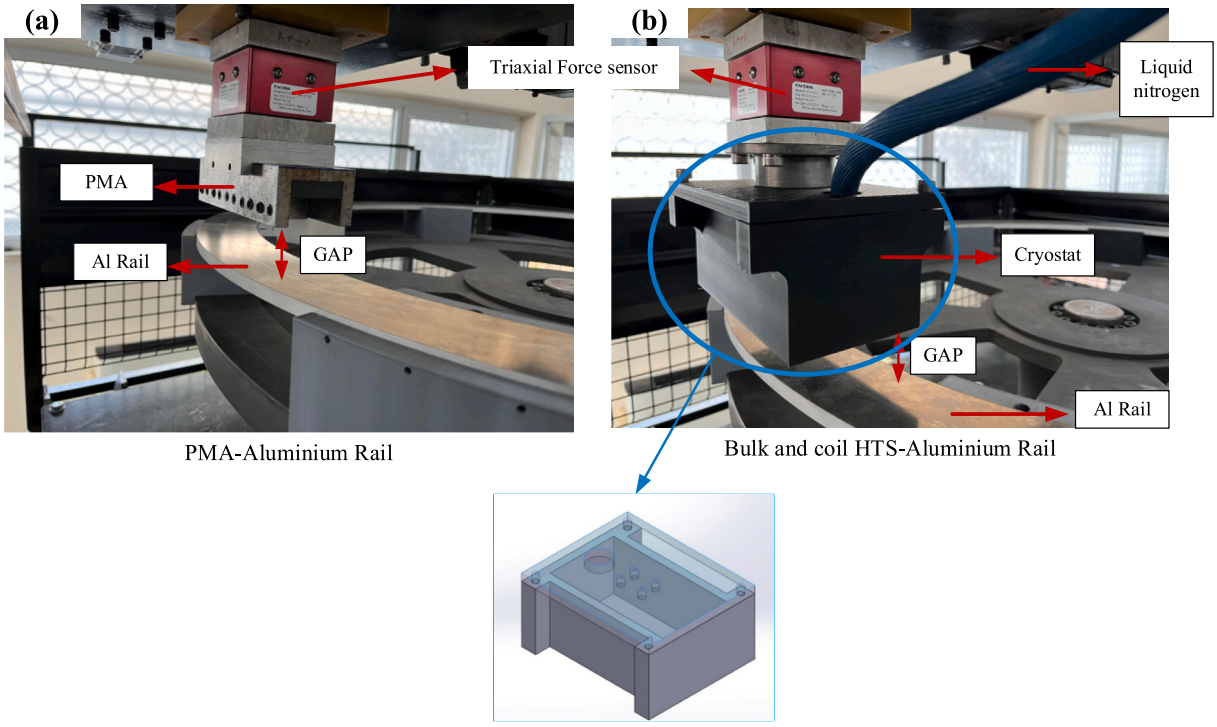

Fig. 3. Different magnetic field sources with PMA (a), bulk HTS and HTS racetrack coil (b) used in the EDL measurement system.

modular and designed to work with different configurations including PMA, bulk HTS, and HTS racetrack coil. In this way, the effects of magnetic field sources on magnetic levitation, guidance force and dynamic behaviour can be analysed comparatively. Images of different magnetic field sources used in the EDL measurement system are given in Fig. 3.

The unit containing the magnetic field source, given in Fig. 3, is designed as a critical component of the dynamic measurement system. Fig. 3(a) shows the magnetic field source module using a PMA, designed for non-cryogenic operation and mounted directly on the positioning unit, while Fig. 3(b) shows the magnetic field source with bulk HTS, placed in a specially designed polylactic acid (PLA)-based cryostat for cryogenic operation. This comparison demonstrates the modularity and adaptability of the system for various magnetic source configurations. At the same time, the triaxial force sensor was assembled on the magnetic field source module. Three different servo motors were used to move the magnetic field source unit in x, y and z axes, and CWDS86C servo motor drivers were preferred to precise position control of these motors. Thanks to closed-loop control, these drivers can control motor movements in real time and correct slip and position errors, thus increasing

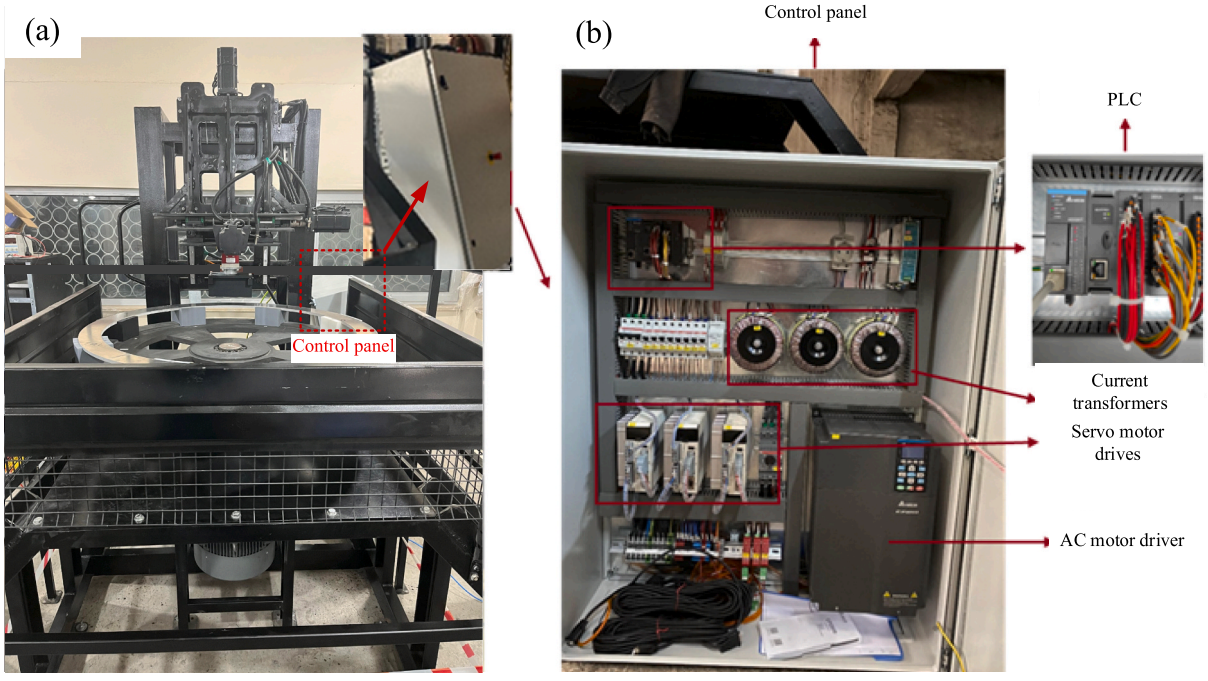

Fig. 4. HTS Maglev EDL measurement system (a) and control panel with PLC (b).

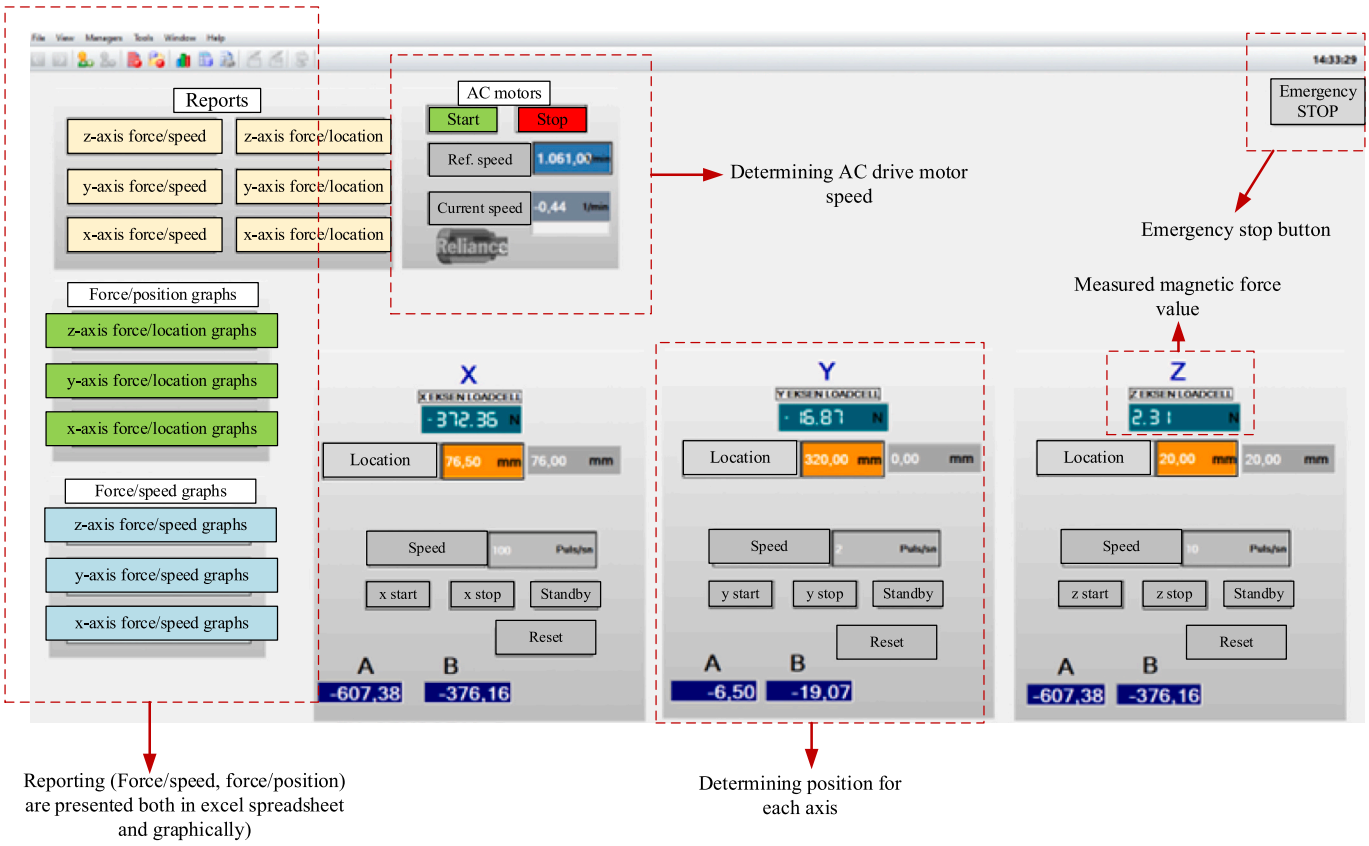

Fig. 5. The designed SCADA interface screen for EDL measurement system.

measurement accuracy. In order to obtain force data in the system reliably, FUTEK MTA400 triaxial force sensor with ± 1N vertical and ± 0.5 N lateral force measurement accuracy, with a maximum measurement capacity of 2200 N in vertical and 1100 N in horizontal is used. This sensor provides high accuracy and precision under dynamic test conditions.

In the dynamic measurement system, a new cryostat was designed to prevent eddy currents that will occur on the lower surface of the aluminium cryostat when the aluminium rail moves at high speeds. This new design, made of PLA material, improves the stability of the system while increasing the accuracy of magnetic field measurements. Fig. 3 shows an overview of the new cryostat.

HTS racetrack coils are used to create a high magnetic field, and an ITECH IT-M3903C-10-340 model high current DC power supply is integrated into the system to meet the high current requirement when used in magnetic field generation. This bi-directional programmable power supply has a voltage of 0–10 V, a max. current of 340A and a power capacity of ± 3.4 kW, allowing magnetic flux density and magnetic force measurements to be performed precisely by applying stable and controlled current HTS racetrack coils.

2.4. Integration of SCADA and PLC to control electrodynamic levitation test system

Fig. 4 shows the position of the control panel in the HTS Maglev dynamic measurement system (a) and detail of the control panel with PLC (b). The integration of SCADA and PLC systems has been realized for the control of the aluminium rail-HTS Maglev dynamic measurement system. Delta AS300 series PLC was chosen for its high-performance modular structure, fast data processing (128 k program steps, 60 k data words) and compatibility with expansion modules (up to 32) and communication protocols (Ethernet, CANopen). The six-axis pulse control capability (200 kHz) ensured precise synchronization of hardware components during dynamic measurements. PLC-SCADA communication is established through the Modbus TCP protocol, chosen for its low latency, reliability and seamless compatibility with existing hardware. This protocol optimized system performance by facilitating seamless data flow between sensors, actuators, drive motors and the controller interface.

The SCADA interface, shown in Fig. 5, allows real-time monitoring and control of magnetic force in all axes at different direction, position and speed parameters. In addition, the addition of an emergency stop button to the SCADA interface increased operational flexibility and safety. Users can adjust motor speeds, monitor live data and terminate operations during abnormalities, which is critical for high-speed Maglev applications.

The SCADA interface designed for the EDL measurement system was created with the PLC software, a section of which is given in Fig. 6. In this section, given as an example, the positioning of the aluminium rail in the z-axis relative to the magnetic field source is provided in the vertical direction. The PLC software allows real-time adjustments and monitoring of the relative position, facilitating accurate and repeatable positioning for experimental studies.

To ensure measurement accuracy, a calibration procedure was performed for the PLC software adapted to the experimental geometry. The Delta AS300 PLC software processed sensor data with appropriate unit conversions and verified positional accuracy through encoder feedback. The calibration involves the using certified reference weights and tachometer verified speed profiles to validate that the force sensor outputs corresponded to actual physical values. Fig. 7 illustrates the force calibration plot in the vertical direction (z-axis) including the resulting function, between measured and actual values. The black solid squares in the figure represent the measured force sensor outputs corresponding to certified reference weights ranging from 10 N to 90 N. The red line indicates the linear regression fit with the equation

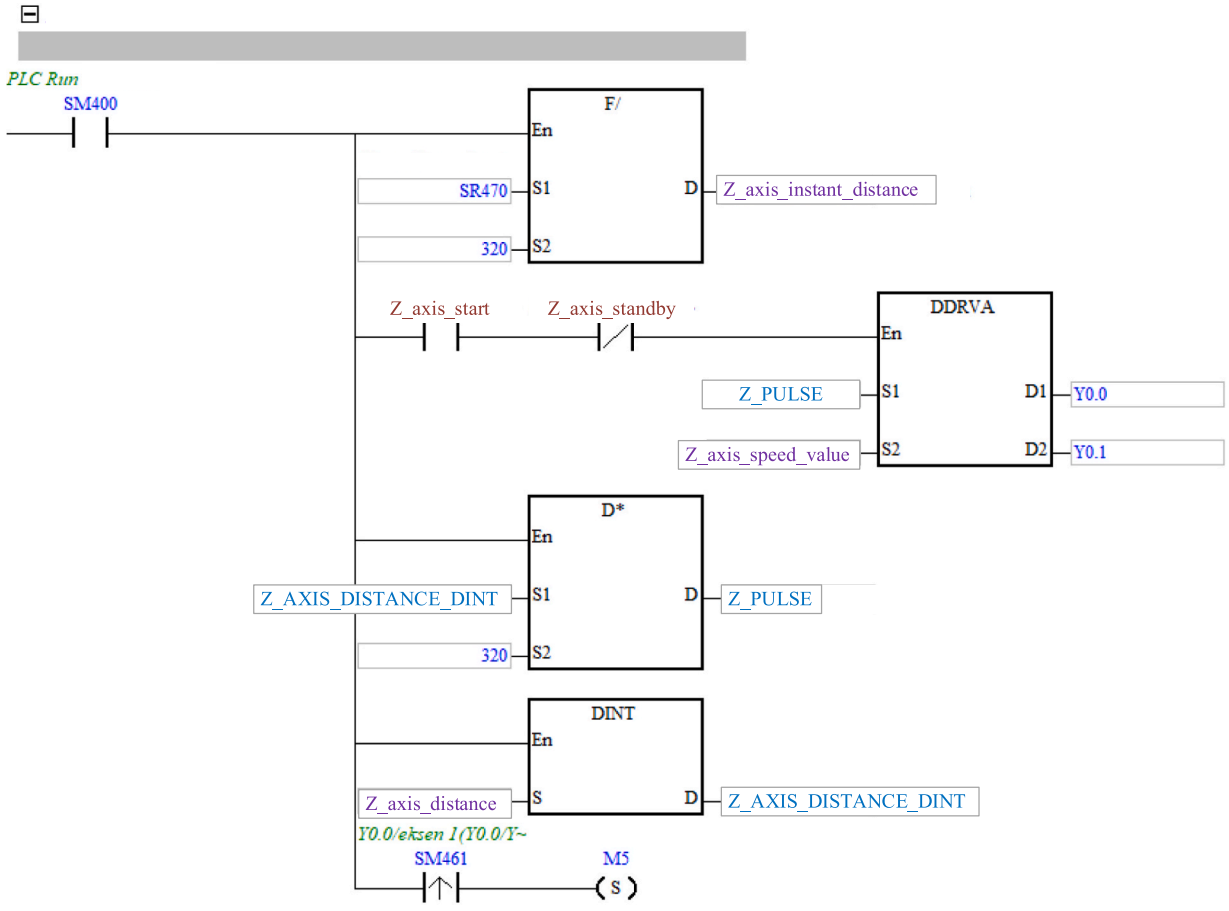

Fig. 6. Z-axis positioning interface of the plc software.

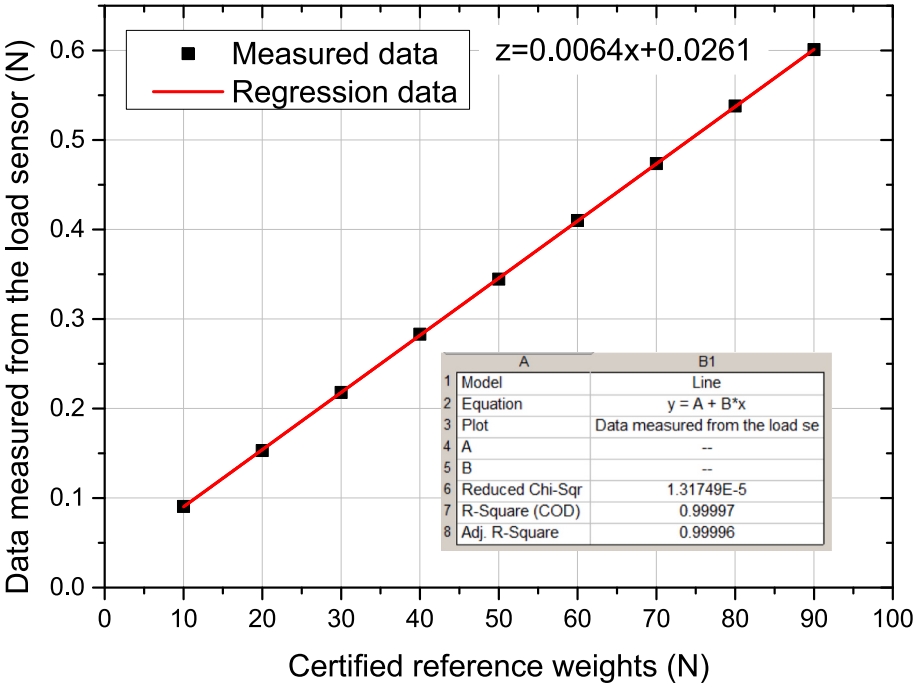

Fig. 7. Triaxial load cell force calibration graph in z-axis.

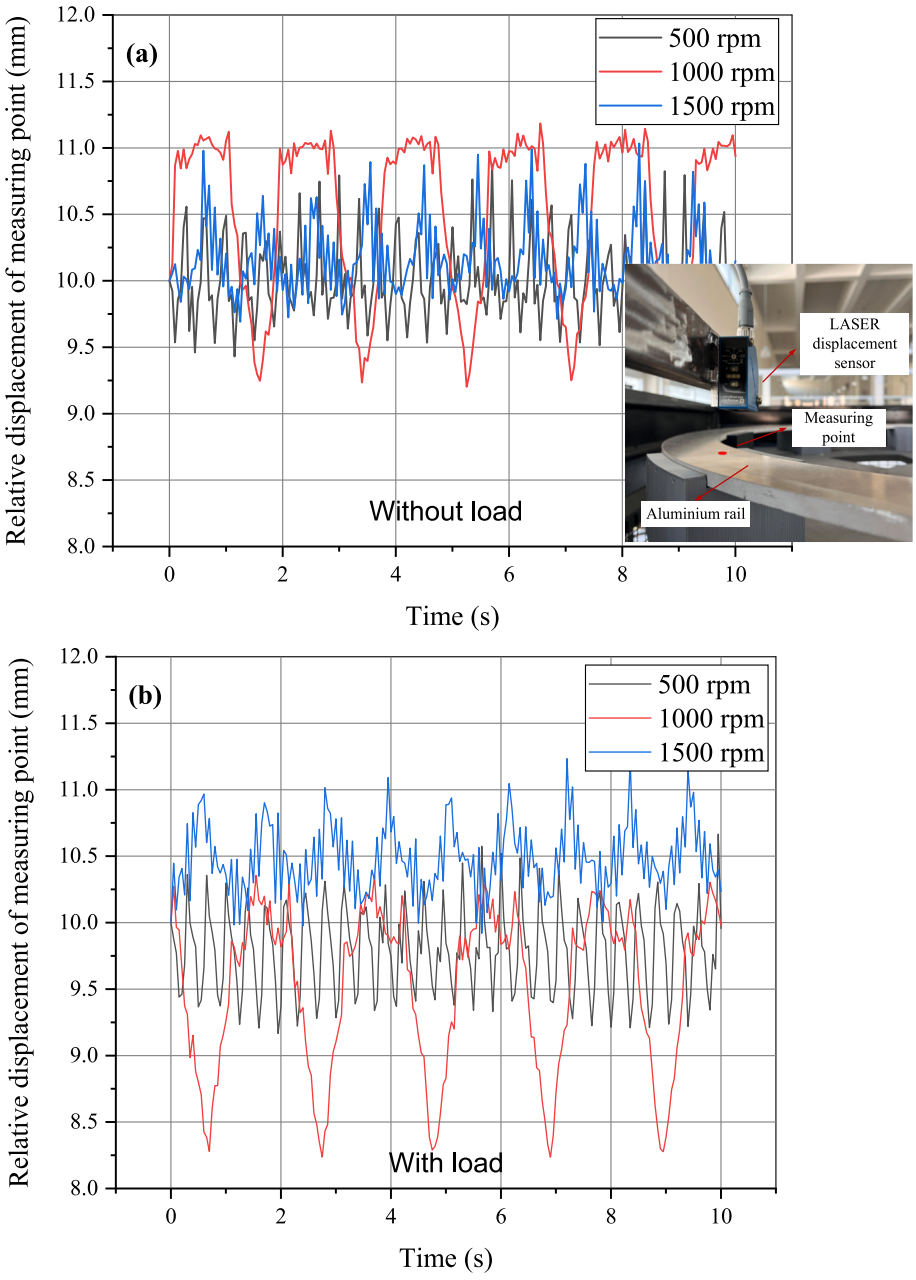

Fig. 8. Vertical displacement of the measuring point in z-axis at various speeds of aluminium rail, without load (a), and with load (PMA) (b). Inset figure (a) shows the measuring point of displacement sensor.

$z = 0.0064x + 0.0261$ and a high coefficient of determination $R^2 = 0.99997$, demonstrating excellent linearity and reliability of the force sensor.

The integration of PLC control and SCADA interface to the high-speed EDL measurement system provides the synchronized control, high-precision measurement and reliable data acquisition required to experimental studies to simulate the real-scale EDL Maglev applications.

3. Experimental verification and discussion

In the high-speed EDL measurement system, the initial measurements focused on determining the vertical displacement of the rotating horizontal aluminium rail system along the z-axis under different operating conditions. For this purpose, a Wenglor brand displacement sensor was integrated to the EDL measurement system.

Firstly, measurements were conducted in the absence of any magnetic field source (see Fig. 2), with displacement data recorded at various rotational speeds (500 rpm = 94 km/h, 1000 rpm = 188 km/h, 1500 rpm = 283 km/h) of the aluminium rail. Subsequently, the same measurements were repeated under the PMA-Aluminium rail configuration, as given in Fig. 3(a). The obtained relative displacement in the z-axis versus time measurement results are presented in Fig. 8. This placement data in this figure was recorded for 10 s just after reaching the maximum rotational speeds of 500, 1000 and 1500 rpm. As shown in Fig. 8, the displacement range in the y-direction in the without load condition was measured as approximately 1.0 mm, 1.8 mm, and 1.1 mm at rotational speeds of 500, 1000, and 1500 rpm, respectively. Under load, these values were measured as 1.0 mm, 2.0 mm, and 1.0 mm, respectively. The fact that the vertical position variations are very close in both loaded and unloaded conditions indicates that the system maintains its previous steady-state position even under load. However, the higher position variation in z-axis measured at 1000 rpm compared

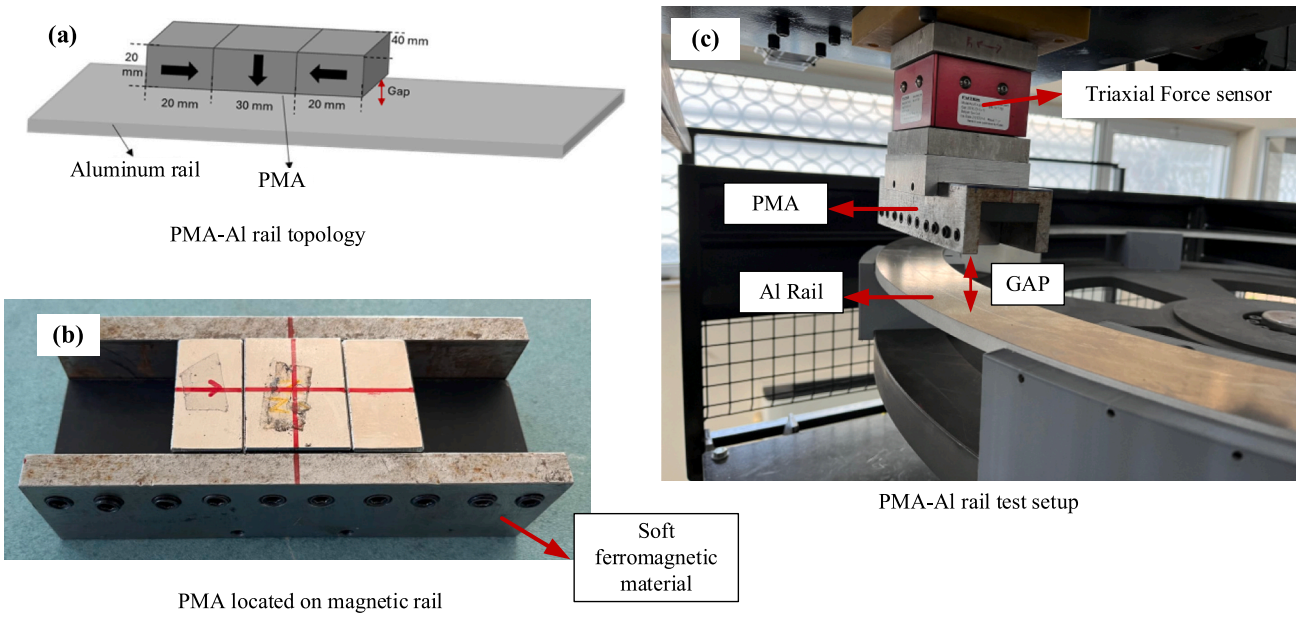

Fig. 9. Detailed PMA-Aluminium rail configuration: schematically view (a) and photo of used PMA (b) and the mounted PMA to the measurement system for magnetic force measurement in the desired vertical gaps (c).

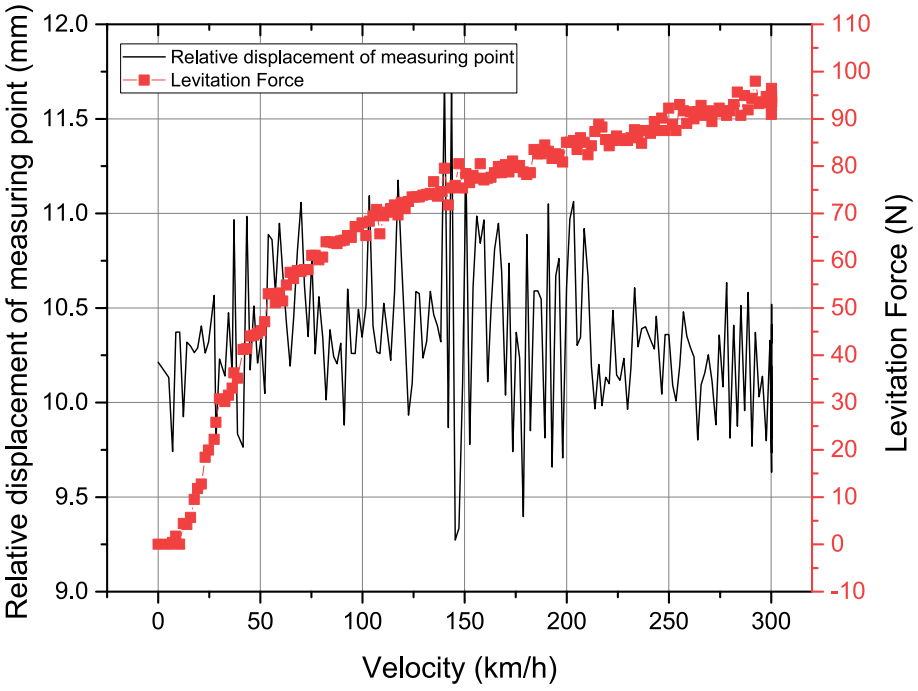

Fig. 10. Levitation force and relative displacement measurements as a function of the velocity.

to other speeds indicated that the manufactured EDL measurement system enters resonance around this rotational speed.

In addition to the change in vertical displacement, another important parameter is the determination of the fluctuation in the magnetic force at high speeds. For this purpose, the measurement setup given in Fig. 9 was created. This figure shows schematically view and photo of used PMA and the mounted PMA to the measurement system for magnetic force measurement in different vertical gaps at different rotational speeds. Levitation force and vertical displacement measurements as a function of velocity are shown in Fig. 10.

For the PMA-Aluminium rail configuration, the relative displacement of the measuring point was measured, and the obtained results are presented in Fig. 10. One can clearly see from Fig. 10 that the levitation force increases rapidly over time depending on the increasing velocity, and as the maximum velocity is approached, the force reaches its maximum value while the increase rate in the force decreases. The fluctuation in the force does not change so much depending on the velocity indicating the stability of force measurements. Around 4–5 N fluctuation is observed in the levitation force curves, but this fluctuation becomes more apparent around 145 km/h (770 rpm), consistent with the change in vertical relative displacement curve around 140–145 km/h. This velocity range indicates that the system reached its first critical speed around this point, due to its natural frequency, at which the system should not be operated for a long time.

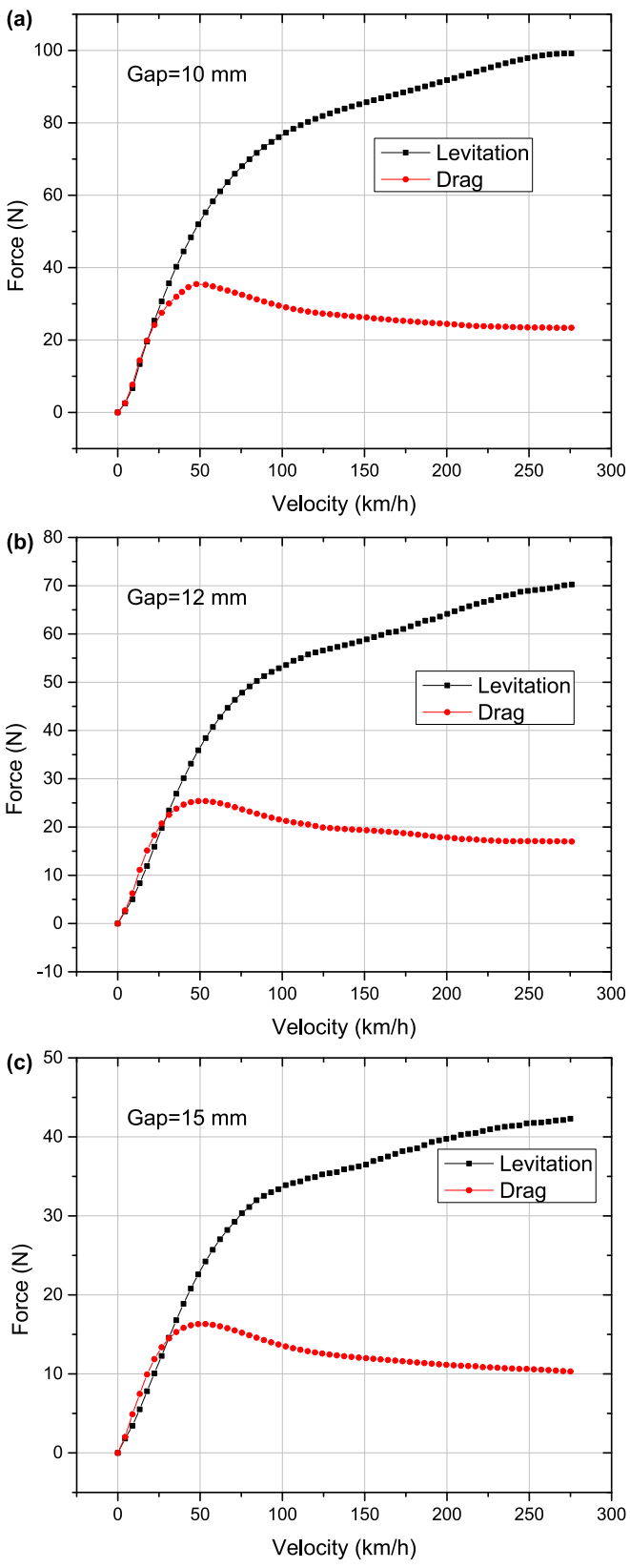

Fig. 11. Levitation and drag force curves in the PMA-EDL system with gaps of 10 mm (a), 12 mm (b), and 15 mm (c) between the PMA and the aluminium rail.

Fig. 11 shows the levitation and drag force curves in the PMA-EDL system at varying gaps between the PMA and the aluminium rail. For all configurations, the levitation force initially increases with velocity, reaching a saturation. This behavior is characteristic of eddy-current-based systems, where induced currents oppose the motion of the PMA according to Lenz's law, resulting in both levitation and drag forces. As the vertical gap increases, the maximum value of the levitation force decreases, indicating reduced magnetic coupling between the magnetic flux of the PMA and the induced current in the aluminium rail. Similarly, the drag force exhibits a peak followed by a plateau, but the overall magnitude diminishes with increasing gap.

Trapped magnetic flux distribution over 2 mm above the HTS surface, which was magnetised by a PMA given in the inset figure (a), and levitation and drag force curves in the bulk HTS-EDL system with gap of 9 mm between the HTS and the aluminium rail (b) is shown in Fig. 12. The maximum magnetic flux density of the PMA over 2 mm above its upper surface is 563 mT while the maximum value of the trapped flux in the HTS is 243 mT. As seen in Fig. 12(b), the levitation force increases with velocity and reaches a saturation after about 150 km/h, while the drag force increases rapidly reaching a peak at about 50 km/h and goes a saturation with increasing velocity.

4. Conclusion

This study presents the development and experimental validation of a high-speed electrodynamic levitation (EDL) measurement system based on the principles of eddy current levitation. The study introduces a modular EDL measurement system designed to investigate the magnetic force between various magnetic field sources and aluminium rail arrangements, and the initial experimental results focused on testing the performance of the system through PMA–aluminium rail and HTS–aluminium rail configurations. The adaptability of the system enables a thorough investigation of how different magnetic field sources influence levitation force, drag force, and dynamic stability at high speeds. A key advancement of this work is the seamless integration of PLC and SCADA systems, which ensures precise synchronization, real-time data acquisition, and controlled experimental execution. Initial experimental results confirmed the system's ability to track vertical displacement variations and levitation force fluctuations across different rotational speeds, reaching up to 1500 rpm. Throughout the tests, the system consistently maintained stable positioning under both loaded and unloaded conditions, with only minor vertical displacement changes observed, except for a slightly increased fluctuation around 1000 rpm (188.4 km/h). For the preliminary tests, levitation forces of 99 N, 70 N and 42 N were measured at different gaps of 10 mm, 12 mm, and 15 mm, respectively, with the PMA at a maximum speed of 1500 rpm, which corresponds to 283 km/h above an aluminium rail. Similarly, maximum levitation force was tested with HTS-aluminium rail configuration as 16 N at the vertical gap of 9 mm.

Using different magnetic field sources with aluminium rails, the developed measurement system is capable of enabling systematic experimental investigations relevant to real-scale EDL applications. Moving forward, efforts will focus on refining system parameters to minimize resonance effects and expanding the testing framework to accommodate additional magnetic configurations and operational conditions. Ultimately, this work contributes to the ongoing advancement of EDL-based maglev technologies by delivering a reliable platform for assessing real-world maglev applications under dynamic conditions.

CRediT authorship contribution statement

U. Kemal Ozturk: Writing – original draft, Supervision, Project administration, Funding acquisition, Conceptualization. **Hakki Mollahasanoglu:** Writing – original draft, Investigation. **Murat Abdioglu:** Writing – original draft, Validation, Investigation. **Halil Ibrahim Okumus:** Writing – original draft, Conceptualization. **Hasan Gedikli:**

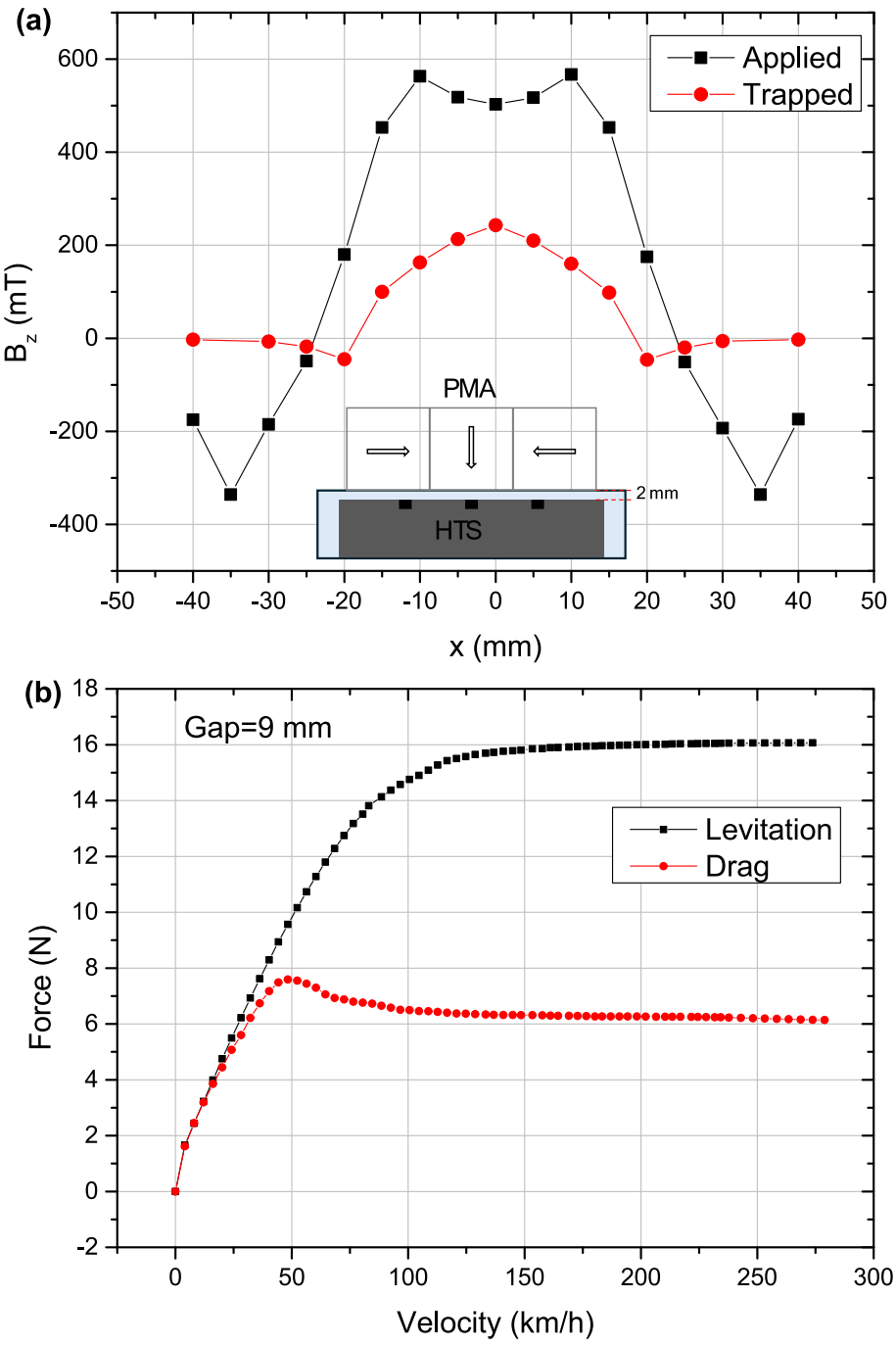

Fig. 12. Trapped magnetic flux distribution over 2 mm above the HTS surface (a) and levitation and drag force curves in the bulk HTS-EDL system with gaps of 9 mm between the HTS and the aluminium rail (b). The inset figure shows the schematic diagram of the magnetic flux trapping setup in the HTS using PMA as magnetic field source.

Writing – original draft, Validation, Conceptualization.

Declaration of competing interest

The authors declare the following financial interests/personal relationships which may be considered as potential competing interests: Ufuk Kemal Ozturk reports financial support was provided by Scientific and Technological Research Council of Turkey. Ufuk Kemal Ozturk reports financial support was provided by Karadeniz Technical University. If there are other authors, they declare that they have no known competing financial interests or personal relationships that could have appeared to influence the work reported in this paper.

Acknowledgements

This study was supported by the Scientific and Technological Research Council of Turkey (TUBITAK) under project number 122F432 and Karadeniz Technical University Scientific Research Projects Coordination Unit under project number FBA-2024-11081.

Data availability

Data will be made available on request.

References

[1] H.W. Lee, K.C. Kim, J. Lee, Review of maglev train technologies, IEEE Trans. Magn. 42 (7) (2006) 1917–1925.
[2] G. Bohn, G. Steinmetz, The electromagnetic levitation and guidance technology of the'transrapid'test facility Emsland, IEEE Trans. Magn. 20 (5) (2003) 1666–1671.
[3] Y. Xu, Z. Zhao, S. Yin, Z. Long, Real-time performance optimization of electromagnetic levitation systems and the experimental validation, IEEE Trans. Ind. Electron. 70 (3) (2022) 3035–3044.
[4] A. Pandey, D.M. Adhyaru, Control techniques for electromagnetic levitation system: a literature review, Int. J. Dyn. Control 11 (1) (2023) 441–451.
[5] U.K. Ozturk, M. Abdioglu, H. Mollahasanoglu, Magnetic force performance of hybrid multisurface HTS maglev system with auxiliary onboard PMs, IEEE Trans. Appl. Supercond. 33 (3) (2023) 1–6.
[6] M.R. Siddiqui, S.M. Ahmad, U. Asghar, Stabilizing control of a 1-DOF electromagnetic levitation of pivoted-free rigid ferromagnetic beam, Measurement 106 (2017) 35–45.
[7] H. Mollahasanoglu, M. Abdioglu, U.K. Ozturk, H.I. Okumus, E. Coskun, A. Gencer, Numerical investigation of EDS maglev systems in terms of performance and cost for different PMs-aluminum rail arrangements, J. Supercond. Nov. Magn. 38 (1) (2025) 52.
[8] L. Wang, Z. Deng, Y. Cheng, A field cooling method to increase the suspension force of HTS pinning maglev system, Cryogenics 123 (2022) 103448.
[9] M. Abdioglu, K. Öztürk, H. Gedikli, M. Ekici, A. Cansız, Levitation and guidance force efficiencies of bulk YBCO for different permanent magnetic guideways, J. Alloy. Compd. 630 (2015) 260–265.
[10] Y. Wen, Y. Xin, W. Hong, C. Zhao, A force measurement system for HTS maglev studies, IEEE Trans. Instrum. Meas. 69 (7) (2019) 5018–5026.
[11] S. Celik, Design of magnetic levitation force measurement system at any low temperatures from 20K to room temperature, J. Alloy. Compd. 662 (2016) 546–556.
[12] L. Schultz, O. de Haas, P. Verges, C. Beyer, S. Rohlig, H. Olsen, U. Funk, Superconductively levitated transport system-the SupraTrans project, IEEE Trans. Appl. Supercond. 15 (2) (2005) 2301–2305.
[13] B. Savaskan, M. Abdioglu, K. Ozturk, Determination of magnetic levitation force properties of bulk MgB2 for different permanent magnetic guideways in different cooling heights, J. Alloy. Compd. 834 (2020) 155167.
[14] W. Hong, Y. Xin, C. Wang, N. Li, A quasi-static measurement method for analyzing the lateral disturbance of HTS Maglev, IEEE Trans. Instrum. Meas. 71 (2022) 1–9.
[15] Z. Deng, H. Shi, Y. Chen, Z. Ke, L. Liang, X. Liu, W. Zhang, A cost-effective linear propulsion system featuring PMEDW for HTS maglev vehicle: design, implementation, and dynamic test, Measurement 240 (2025) 115618.
[16] D. Zhou, C. Cui, L. Zhao, Y. Zhang, X. Wang, Y. Zhao, Static and dynamic stability of the guidance force in a side-suspended HTS maglev system, Supercond. Sci. Technol. 30 (2) (2016) 025019.
[17] L. Liu, J. Wang, Z. Deng, J. Li, J. Zheng, G. Ma, S. Wang, Levitation force transition of high-Tc superconducting bulks in varying external magnetic field, IEEE Trans. Appl. Supercond. 20 (3) (2010) 920–923.
[18] P.J. Zhuo, Z.X. Zhang, X.F. Gou, Chaotic motion of a magnet levitated over a superconductor, IEEE Trans. Appl. Supercond. 26 (2) (2016) 1–6.
[19] Z. Deng, J. Li, W. Zhang, Y. Gou, Y. Ren, J. Zheng, High-temperature superconducting magnetic levitation vehicles: dynamic characteristics while running on a ring test line, IEEE Veh. Technol. Mag. 12 (3) (2017) 95–102.
[20] J. Wang, S. Wang, C. Deng, Y. Zeng, L. Zhang, Z. Deng, Y. Zhang, A high-temperature superconducting maglev dynamic measurement system, IEEE Trans. Appl. Supercond. 18 (2) (2008) 791–794.
[21] K. Ozturk, A. Badía-Majós, M. Abdioglu, D.B. Dilek, H. Gedikli, Experimental and numerical investigation of levitation force parameters of novel multisurface Halbach HTS–PMG arrangement for superconducting Maglev system, IEEE Trans. Appl. Supercond. 31 (7) (2021) 1–12.
[22] S. Zhang, Z. Deng, Z. Huang, H. Li, X. Zhou, W. Zhang, Measurement of levitation force of high-temperature superconducting maglev under high-speed operation condition, Cryogenics 139 (2024) 103808.
[23] Z. Wang, H. Yang, W. Lei, J. Zheng, Multi-parameter refinement mechanical properties measurement of high temperature superconducting bulk array for maglev system, Measurement 251 (2025) 117249.
[24] N. Qian, J. Zheng, W. Lei, B. Wang, J. Li, Y. Ren, Z. Deng, Dynamic vibration characteristics of HTS levitation systems operating on a permanent magnet guideway test line, IEEE Trans. Appl. Supercond. 27 (4) (2017) 1–5.
[25] E. Tramacere, M. Pakštys, R. Galluzzi, N. Amati, A. Tonoli, T.A. Lembke, Modeling and experimental validation of electrodynamic maglev systems, J. Sound Vib. 568 (2024) 117950.
[26] S. Kusada, M. Igarashi, K. Nemoto, T. Okutomi, S. Hirano, K. Kuwano, M. Yamaji, The project overview of the HTS magnet for superconducting maglev, IEEE Trans. Appl. Supercond. 17 (2) (2007) 2111–2116.
[27] Y. Wen, Y. Xin, W. Hong, C. Zhao, W. Li, Comparative study between electromagnet and permanent magnet rails for HTS maglev, Supercond. Sci. Technol. 33 (3) (2020) 035011.
[28] H.S. Han, D.S. Kim, Magnetic levitation, Springer Tracts on Transportation and Traffic, Springer, Netherlands, 2016, p. 247.